UNIVERSITY OF ZIELONA GÓRA

CIVIL AND ENVIRONMENTAL ENGINEERING REPORTS

E-ISSN 2450-8594

CEER 2026; 36 (1): 0039-0060
DOI: 10.59440/ceer/217451

Original Research Article

AUTOMATED DETECTION OF ASBESTOS-CEMENT ROOFS USING MULTI-SOURCE REMOTE SENSING DATA AND MACHINE LEARNING

Kacper DURCZAK, Joanna JANICKA *, Wioleta BŁASZCZAK-BĄK
Faculty of Geoengineering, Department of Geodesy, Universtity of Warmia and Mazury in Olsztyn, Poland

A b s t r a c t

Asbestos, due to its resistance to temperature, chemicals, and mechanical damage, was widely used in construction, especially in the second half of the 20th century. Today, most of the remaining asbestos products are roofing sheets, which pose a serious health risk and the WHO calls for its elimination. One of the key actions is to identify buildings with asbestos-cement roofing. As part of the research, a method for detecting such buildings was developed using machine learning, LiDAR technology, orthophotos, and satellite images. The developed model is based on data such as reflection intensity, roof slope, and year of construction. The proposed methodology allows for the effective localization of buildings covered with this hazardous material. The model successfully identified between 79% and 91% of asbestos-covered buildings across three diverse test areas, and up to 90% of buildings were correctly classified in terms of roofing material. Quantitative evaluation demonstrates that the proposed method effectively identifies asbestos-covered buildings achieving precision values ranging from 0.59 to 0.89 and recall between 0.77 and 0.86. The resulting F1-scores (0.70–0.88) confirm a strong balance between correct and false detections. Detection accuracy was influenced by environmental factors such as tree coverage and surface contamination, which introduced visual noise in RGB imagery and occasionally led to misclassification. Despite these limitations, the results confirm the high potential of this approach for asbestos detection. The study demonstrates that integrating LiDAR intensity, roof geometry, and visual data significantly improves the reliability of asbestos-cement roof identification compared to single-source methods.

Keywords: asbestos, machine learning, LiDAR

* Corresponding author: Joanna Janicka University of Warmia and Mazury in Olsztyn, Poland, Oczapowskiego 2 10-719 Olsztyn, joannasuwm@gmail.com, 89 523-42-04

1. INTRODUCTION

Asbestos is a group of naturally occurring silicate minerals that form thin, fibrous crystals. In its natural state, asbestos resembles rock; however, once property processed, it exhibits exceptional properties such as high resistance to heat, fire, chemicals, and mechanical wear, as well as effective soundproofing and thermal insulation. These characteristics contributed to the widespread use of asbestos in construction and industry throughout much of the 20th century, particularly during the 1960s and 1970s [1,2]. There are several types of asbestos, with the most common being chrysotile (white asbestos), amosite (brown asbestos), and crocidolite (blue asbestos). Among them, chrysotile, classified within the serpentine group, is estimated to account for more than 90% of the total global asbestos usage [3–5].

Asbestos-containing materials were used extensively in buildings (e.g., roofing, wall cladding, and insulation), in infrastructure (e.g., sewage pipes), and across various industries including shipbuilding, the automotive industry (brake and clutch linings), as well as some household products [5].

Despite its utility, asbestos has proven to be extremely hazardous to human health. Its microscopic fibers can easily become airborne, especially when asbestos-containing materials are damaged or improperly handled and are readily inhaled. Once inside the lungs, these fibers can cause severe and often fatal diseases, such as asbestosis, lung cancer, and mesothelioma. Critically, these diseases often manifest decades after exposure, making early diagnosis and treatment challenging [1,6]. Due to these health risks, asbestos is now classified as a hazardous material.

In Poland, the production and use of asbestos have been completely banned since 1999. In response, a national program for the systematic removal of asbestos-containing products has been implemented, with a target completion date set for December 31, 2032, [3,7]. According to this program, all asbestos materials must be removed by certified companies using appropriate protective equipment and disposal protocols. A key challenge, however, remains the identification of asbestos in existing structures, particularly in rural or poorly documented areas where asbestos-cement materials such as eternit are still prevalent.

Eternit was particularly popular as a roofing material due to its strength, fire resistance, moisture resistance, and durability. It was produced in two main forms: corrugated sheets (with small or large waves) and flat tiles. Because these materials visually resemble non-asbestos alternatives, their identification often requires specialist knowledge or laboratory testing [8,9]. Examples of asbestos-cement roof coverings are presented in Figure 1.

(a) (b)

Fig. 1. Roof covered (a) with corrugated asbestos, (b) with flat asbestos

Given that the presence of asbestos must be reliably identified before any renovation or demolition work, there is an urgent need for efficient, scalable, and non-invasive detection methods. Traditional manual inspections are time-consuming, costly, and often logistically unfeasible for large areas. Consequently, modern technologies based on remote sensing and machine learning offer a promising solution.

Over the past two decades, a variety of methods have been developed to address the challenge of locating and classifying asbestos-cement roofs. These approaches can be broadly divided into three categories: in-situ field inspections, laboratory analyses, and remote sensing-based techniques. These approaches include the following:

1. Field inspections and laboratory testing

Traditionally, the identification of asbestos materials has relied on on-site visual inspections performed by trained professionals, followed by laboratory confirmation using techniques such as Polarized Light Microscopy (PLM), X-ray diffraction (XRD), or Scanning Electron Microscopy (SEM). While accurate, these methods are labor-intensive, time-consuming, and generally not feasible for large-scale surveys. Moreover, visual inspection alone can be unreliable due to the difficulty in distinguishing asbestos-cement products from visually similar materials without destructive sampling [1,2].

2. Spectral and thermal imaging approaches

Several studies have explored the use of hyperspectral imaging and Thermal Infrared (TIR) data to detect asbestos-containing materials based on their unique spectral or thermal signatures. Hyperspectral sensors, which capture reflectance data across hundreds of narrow wavelength bands, can sometimes identify characteristic features of asbestos-cement, especially under controlled conditions [9,10]. However, the availability of high-resolution hyperspectral data is limited, and such systems are expensive and often impractical for arge-scale monitoring.

3. Aerial and satellite remote sensing

The most scalable methods for asbestos detection rely on aerial orthophotos, multispectral satellite imagery, and increasingly Light Detection and Ranging (LiDAR) data. High-resolution orthophotos (with resolutions of 10–25 cm per pixel or better) can be used to visually or algorithmically distinguish roof materials based on texture, color, and shape. Some studies have used manual interpretation, while others apply supervised image classification or machine learning techniques [5,11]. Multispectral satellite imagery, such as from WorldView or Sentinel-2 satellites, has also been used in combination with spectral indices or classification algorithms to infer roofing material types, although accuracy may be limited by spatial resolution and atmospheric effects [12].

4. LiDAR and 3D data analysis

LiDAR data, which captures 3D point clouds of urban or rural environments, can provide valuable structural information such as roof slope, orientation, and surface roughness, thereby supporting the distinction of asbestos-cement sheets from other roofing types. When combined with orthophotos or satellite imagery, LiDAR enhances classification performance by adding geometric features to spectral or textural analysis [13].

5. Machine learning and deep learning approaches

Recent advances have focused on machine learning (ML) and deep learning (DL) models trained on remote sensing data to detect asbestos-cement roofs. Studies have used models such as Random Forest, Support Vector Machines (SVMs), and more recently, Convolutional Neural Networks (CNNs) for image classification. CNNs, in particular, have demonstrated strong performance in identifying asbestos-cement roofs when trained on annotated datasets derived from orthophotos or drone imagery [14,15]. These models can automatically learn spatial and visual patterns associated with asbestos-cement materials, offering both accuracy and scalability.

Despite the promising results, challenges remain with respect to generalizability across regions, sensitivity to lighting and weather conditions, and the availability of high-quality training datasets. Therefore, there is a growing interest in multi-source data fusion (e.g., combining LiDAR, multispectral images, and aerial photos) to improve detection accuracy and reliability on a national scale.

The pressing need to meet the national asbestos removal deadline, combined with the health risks posed by unidentified asbestos materials, constitutes the central motivation for this research. Poland still has hundreds of thousands of buildings containing asbestos-based roofing, especially in rural areas, where accurate and comprehensive identification remains a significant logistical and administrative challenge. Automating the identification process using modern geospatial data and machine learning methods can accelerate inventory efforts and support public health and environmental safety initiatives.

Unlike previous studies that typically relied on a single data source, such as spectral information from hyperspectral imagery, textural cues from orthophotos, or geometric attributes extracted from LiDAR point clouds, this study introduces a multi-source fusion approach that integrates LiDAR intensity, elevation-derived roof geometry, and high-resolution orthophoto features within a single, coherent machine learning framework. Prior work often focused either on visual classification or spectral discrimination alone, whereas the proposed method simultaneously leverages radiometric, spatial, and structural characteristics of roofing materials.

This multi-source fusion strategy represents a novel contribution by enhancing classification robustness across diverse environmental condition and improving the ability to distinguish asbestos-cement roofs from visually similar non-asbestos materials, addressing key limitations reported in earlier research. Moreover, the study provides a reproducible workflow applicable to large-scale national inventories, offering practical value for environmental monitoring and policy implementation.

The main objective of this study is to develop an automated method for the identification of asbestos-cement roofing (e.g., eternit) using remote sensing data and machine learning techniques. To achieve this, the study focuses on the following specific objectives:

1. Utilize multiple geospatial data sources – including LiDAR point clouds, high-resolution orthophotos, and satellite imagery – to extract information relevant to roof material classification.
2. Apply and evaluate machine learning models capable of detecting asbestos-cement roofs based on textural, spectral, and geometric features.
3. Create an algorithm that enables large-scale, automatic roof analysis suitable for regional and national implementation.
4. Provide a decision-support tool that assists administrative units in registering asbestos-containing buildings and planning safe removal strategies.

By combining state-of-the-art image processing, machine learning, and geospatial analysis, this approach aims to significantly improve the efficiency and reliability of asbestos identification in Poland and potentially in other regions.

2. METHODOLOGY

The proposed methodology for the effective localization of buildings covered with asbestos is presented in Figure 2.

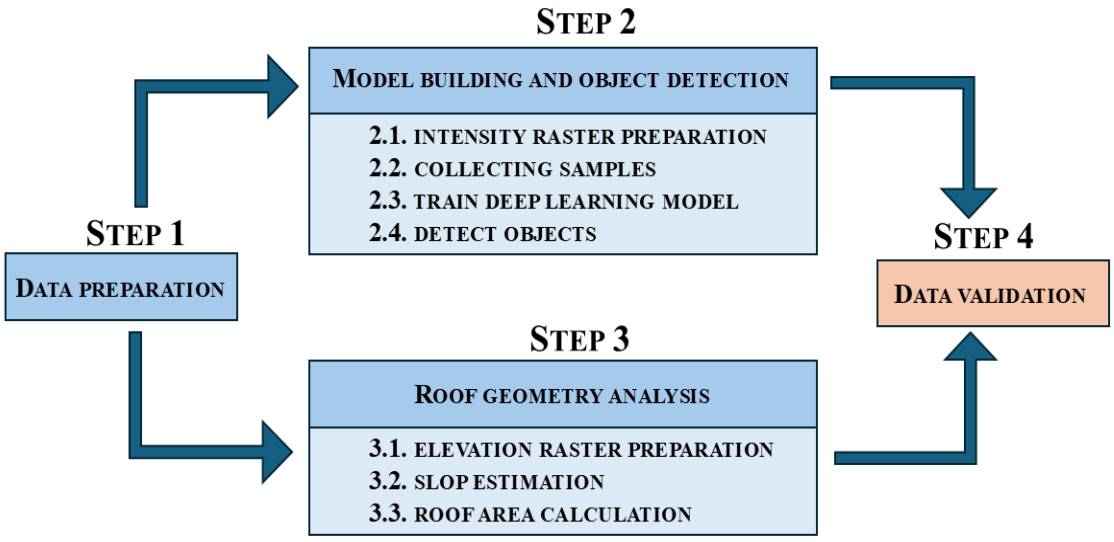

Fig. 2. Graph of the methodology

According to the methodology presented in Figure 2, the following research steps were planned as part of the study:

STEP 1. Data preparation – downloading Airborne Laser Scanning (ALS) point clouds from the geoportal.gov.pl, data filtering and merging the point cloud into a single file.

STEP 2. Model building and object detection

STEP 2.1. Intensity raster preparation – converting the point cloud into a raster representing reflection intensity values of a given pixel size and exporting it to the TIFF format with the RGB mode enforced in order to enable sample collection and object detection.

STEP 2.2. Collecting samples – using the "Label Objects for Deep Learning" function on the obtained raster to mark buildings covered with asbestos. After selecting the appropriate data format, the algorithm will create a directory on the disk containing samples from the studied area. This operation is repeated for subsequent rasters until the desired number of samples is obtained

STEP 2.3. Train deep learning model – using the "Train Deep Learning Model" function and the obtained samples to create a model with predefined parameters.

STEP 2.4. Detect objects – using the "Detect Objects Using Deep Learning" function, the algorithm searches for asbestos-cement roofs in the remaining raster data.

STEP 3. Roof geometry analysis

STEP 3.1. Elevation raster preparation and slope estimation – converting the point cloud into a raster representing building heights and exporting it to the TIFF format without enforcing RGB mode. Using the "Slope" function, roof slopes are estimated from the resulting rasters.

STEP 3.2. Roof area calculation – performing zonal statistic to calculate the horizontal roof areas.

STEP 3.3. Using the calculated parameters to estimate roof slope.

STEP 4. Data validation – verifying whether the buildings detected as asbestos-covered are indeed asbestos-containing, based on additional parameters such as year of construction, roof slope or visual features, as well as field surveys and analysis of archival photographs.

The collection of samples is a vital phase in any data-driven project, as it provides the foundation for developing an effective model. By gathering representative samples, it becomes possible to identify relevant patterns and prepare reliable training data. In this study, samples were obtained through the analysis of filtered point clouds and derived rasters. To increase verification accuracy, Google Street View was used to confirm the presence of asbestos-covered roofs. This was particularly important because the available LiDAR data was collected mainly between 2012–2019, meaning that field conditions may have changed. Archival street-level imagery enabled more precise verification, significantly improving the reliability of the sample collection process.

Training deep learning model (STEP 2.3) constitutes the most critical stage of the workflow. Machine learning involves training algorithms to recognize patterns in data and make predictions without explicit rule-based programming. At this phase, the model is exposed to samples, enabling it to learn patterns and features through iterative adjustments of its internal parameters. Through iterative learning, the model progressively improves its ability to recognize similar data across different datasets; for example, by using samples from one raster, the model can identify similar objects in other rasters. Once trained, the model generalizes these learned patterns to new, unseen data, enabling automated classification, detection, or regression tasks [17].

Asbestos-cement roofing materials show characteristic ranges of reflectance intensity values, making them suitable features for use in machine learning process. Based on these features, a classification model can be developed to automatically detect asbestos-containing roof coverings. This approach substantially accelerates the identification process and increases its precision and reliability. Additional background information on the Geographic Information System (GIS) tools used in the study is provided in Appendix 1.

3. RESULTS

3.1. Data preparation – STEP 1

The analysis was conducted on selected objects located in the Lublin Voivodeship, in the eastern part of Poland. The locations of tested objects and training samples are presented in Figure 3.

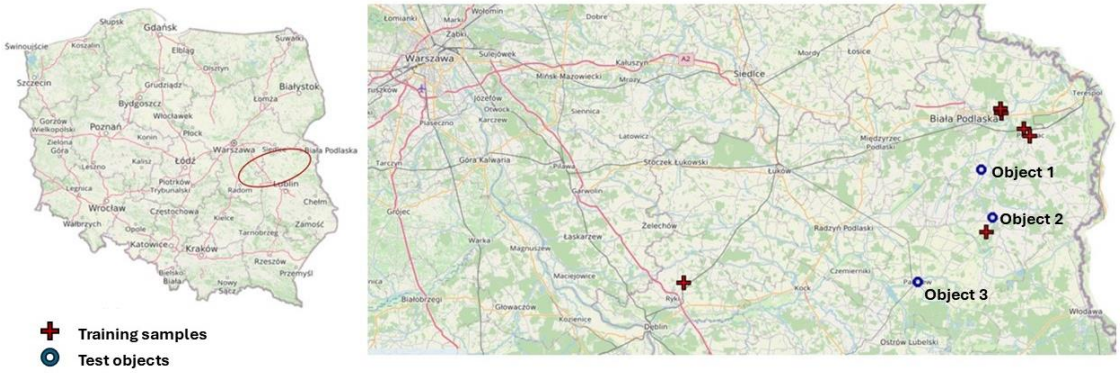

Fig. 3. Localization of tested objects and training samples

Detection of asbestos was carried out for three selected test objects: Łomazy (Object1), Wisznice (Object2) and Parczew (Object3). The objects were selected by analyzing the availability of archival data on Google Maps service, which significantly facilitated data validation. These objects are also characterized by a high concentration of roofs covered with materials containing asbestos, which facilitated the acquisition of samples. Training samples (marked in Figure 3 with red crosses) were collected from the following localities: Rososz (Sample1), Chotyłów (Sample2), Woskrzenice Małe (Sample3), Woskrzenice Duże (Sample4), Horodyszcze (Sample5), and Piszczac (Sample6).

The data were obtained from the geoportal.gov.pl website (accessed on November 21, 2024) as ALS point clouds in PL-KRON86-NH reference system in LAZ format. KRON86 was chosen instead of the currently used EVRF2007 because it covers the entire area of Poland, whereas EVRF2007 is not yet available in the eastern regions of Poland [24].

3.2. Model building and object detection - STEP 2

Building modeling and object detection constitute a stage consisting of several steps. It requires the preparation of an intensity raster, sample collection, training a deep learning model, and final detection of objects based on the selected features.

3.2.1. Intensity raster preparation and samples collecting

The study used LiDAR data, which allow to acquisition of point cloud representing objects such as buildings, trees, and other landscape elements [16].

LiDAR determines the position of objects by measuring the time of flight of emitted laser pulses. The recorded intensity represents the amplitude of the reflected signal and depends on surface reflectivity, the angle of incidence of the laser beam, and the material properties. These physical factors generate characteristic intensity patterns that can be used for material classification. The output data (point cloud) consist of the 3D coordinates (X, Y, Z) of the measured points together with reflection intensity. Different materials – such as metal, wood, asbestos-cement (eternit), and ceramic roof tiles – reflect the laser signal to different degrees. Analysis of the intensity of the reflection allows improved differentiation of roofing types and other structures. This is especially useful in identifying buildings that contain asbestos, where traditional visual methods are sometimes insufficient [13].

Asbestos-cement sheets, due to their rough surface, darker color, frequent biological contamination (such as lichens and mosses), and often characteristic corrugated shape, typically show lower reflection intensity compared to ceramic or metal roof tiles. These features cause the laser beam to be more dispersed or absorbed and less efficiently reflected to the sensor. As a result of these differences in signal intensity, it is possible to more effectively recognize asbestos-cement roofs using LiDAR data, especially when analyzed in combination with other spatial information such as orthophotos or satellite images [17]. Some reference roofs are shown in Figure 4.

Fig. 4. An example of non-asbestos-cement roofs (left) and asbestos-cement roofs (right)

From the training dataset Sample1 all roofs identified as being covered with asbestos were selected. For these reference roofs, an analysis of the intensity parameter was conducted. Figure 5 presents the intensity values for buildings with asbestos and non-asbestos-cement roof collected from training samples. The training dataset consisted of about 1400 samples ensuring sufficient representation of roofs with varying degrees of surface degradation and illumination conditions.

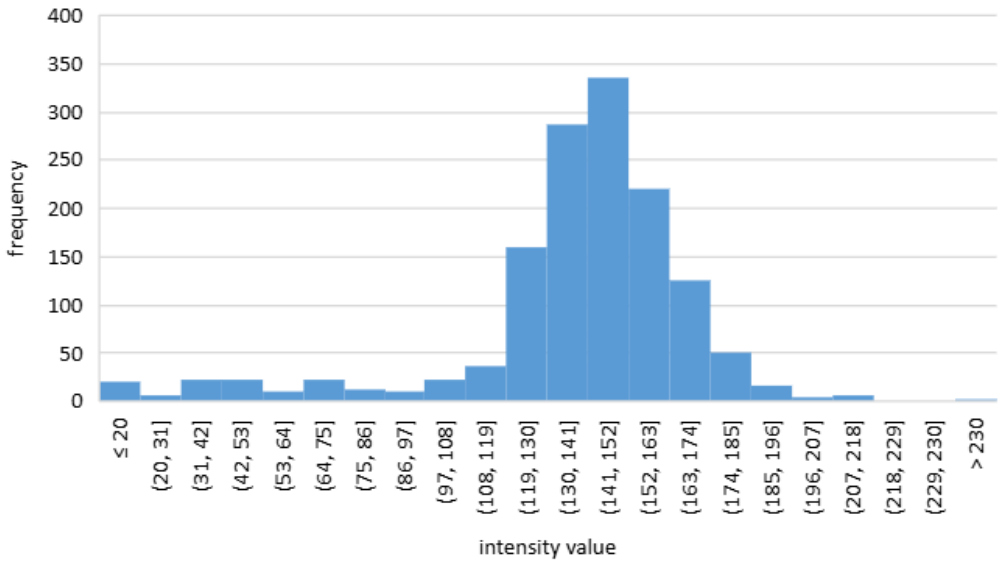

Fig. 5. Reflection intensity histogram

Analyzing the graphs presented in Figure 5, it can be concluded that asbestos covered roofs possess characteristic average values of reflection intensity (110 –160), with can be used to differentiate them from other roofing materials, such as metal sheets or ceramic tiles. The point clouds were converted into rasters using the "LAS Dataset to Raster" function. The reflectivity intensity (Intensity) was selected as the attribute value (Value Field) to obtain a raster representing these values. The Sampling Value (SV) was set to 0.35, which ensured an appropriate data density. Higher values (0.4–0.5) resulted in an excessively sparse distribution of intensity information, while lower values (0.1–0.2) led to the occurrence of numerous "holes" in the raster, which made further analysis difficult. The final raster was exported to the TIFF format with the RGB mode enforced. As a result, the resulting TIFF file contained three channels (red, green, blue), which allowed its use both for sample collection and object detection. One of the raster layers generated for Object1 is presented in Figure 6.

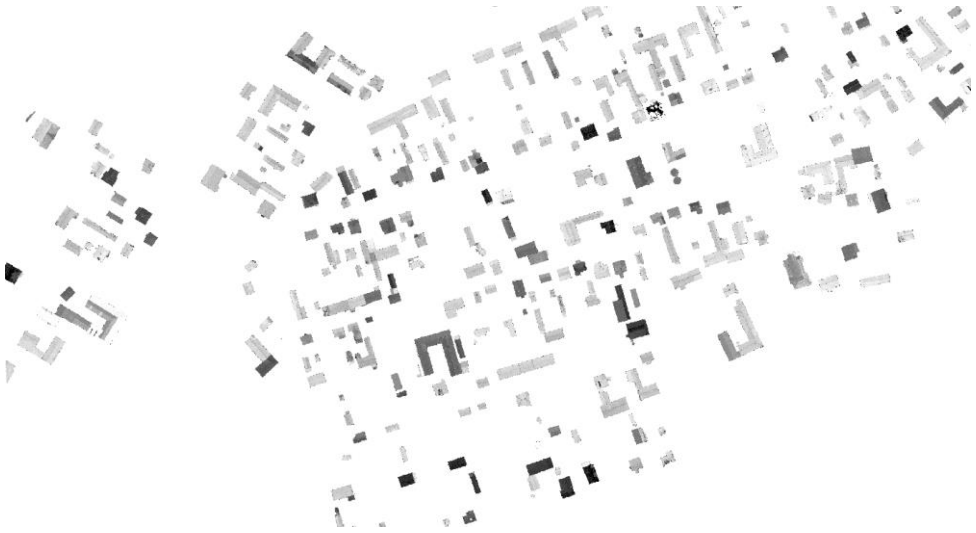

Fig. 6. An example of intensity raster

This raster was generated from the intensity data of Object1, in accordance with the methodology described above. Darker colors represent higher values of reflection intensity.

3.2.2. Train Deep Learning Model

The following Table 1 summarizes the specific parameters and their values used in the conducted research. Appendix 2 presents information that may be crucial for the selection and analysis of parameters used in the evaluation of roof coverings. Each row of the table describes one of the parameters that can be set or adjusted during the training of the neutral network model. These parameters concern different aspects of the machine learning process.

Table 1. Parameters used during machine learning model training

Parameter Name	Description
Meta Data Format	PASCAL Visual Object Classes – one of the most popular metadata formats used in machine learning, mainly in tasks such as image classification, object detection or semantic segmentation. This format describes information about images and objects in them. Data is saved in XML files, according to a set structure.
Max Epochs	20
Model Type	FasterRCNN – used in object detection
Batch Size	8
Validation %	20%
Chip Size	256
Learning Rate	unspecified value – the optimal learning rate was extracted from the learning curve during the training process.
Backbone Model	ResNet-101 – The pre-configured model will be a residual network trained on the Imagenet dataset, which contains over 1 million images and has 101 layers of depth.

Monitor Metric	Validation Loss – the validation loss will be monitored. Once the validation loss no longer changes significantly, the model will be stopped.
Weight Initialization Scheme	Random – random weights will be initialized for non-RGB bands, while the pre-trained weights will be retained for RGB bands.
Freeze Model	Random – random weights will be initialized for non-RGB bands, while the pre-trained weights will be retained for RGB bands.

The Figure 7 shows the training and a validation loss curve for a deep learning model. Two curves can be observed: blue and orange. The blue line represents the training loss as the number of batches processed increases, whereas the orange line represents the validation loss. Both losses decrease rapidly at the beginning (during the first few hundred batches), indicating that the model is learning and improving. At the beginning, the loss function is very high, which is typical for newly initiated training. As training progresses, the loss on the training set decreases quickly and stabilizes at a low value. The loss on the validation set also decreases but remains slightly higher than that of the training set. After approximately 500 batches, both the training and validation curves stabilize, indicating that the model has achieved a balance between learning and generalization. The absence of a sharp increase in validation loss suggests that there is no significant overfitting. This indicates that the model is expected to perform with comparable accuracy on both the training data and previously unseen data. In the case of overfitting, the model learns not only the relevant patterns but also noise, errors, and random relationships that are present only in the training dataset.

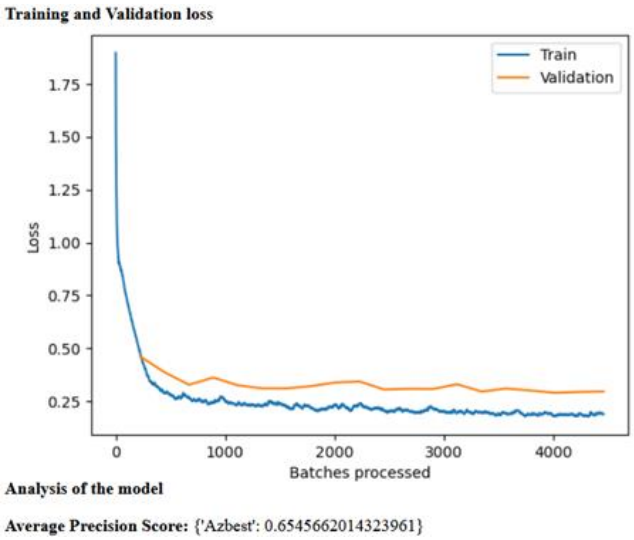

Fig. 7. Graph of the obtained model

The average precision (AP) score for the model is provided below the graph. The score for detecting asbestos is approximately 0.6546 (where the maximum possible value of the average precision score is 1.0), which provides an indication of the model's precision in identifying asbestos-related features in the data.

3.2.3. Detect objects

The trained model was used to detect asbestos-cement roofs on three objects, and the results are presented in Figure 8 – 10.

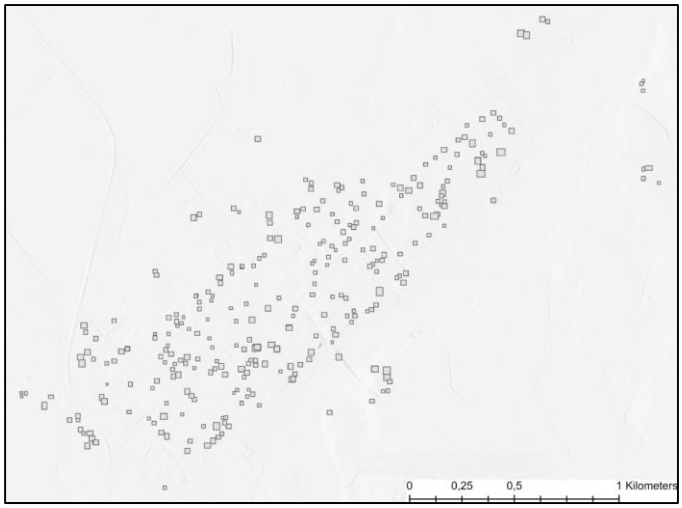

Fig. 8. Detection results for Object1

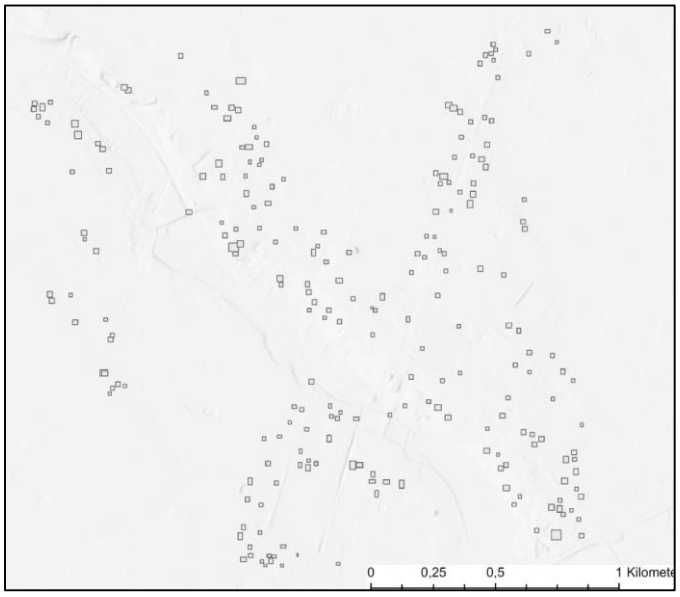

Fig. 9. Detection results for Object2

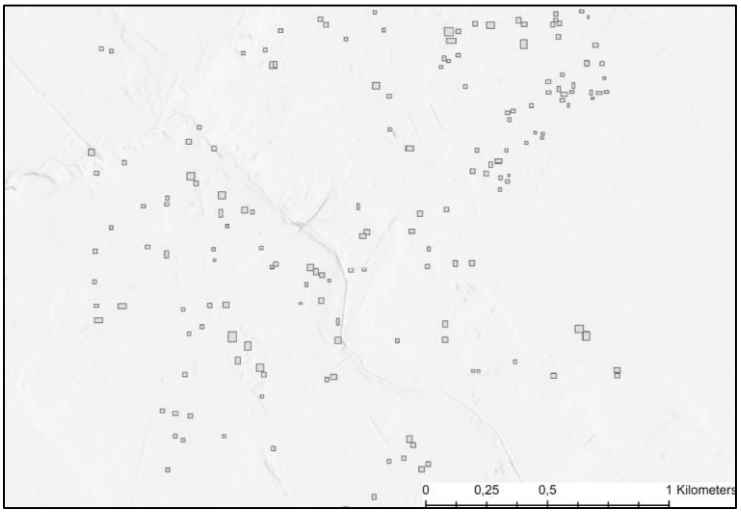

Fig. 10. Detection result for Object3

As part of the conducted analysis of asbestos-cement roof detection using AI-based methods, the following results were obtained: 341 roofs were identified in Object1, 243 in Object 2, and 175 in Object 3.

4. Roof geometry analysis – STEP 3

STEP 3.1 of the roof geometry analysis involves creating a raster representing elevation values. This can be achieved in a relatively simple way: when converting the LAS file to raster format using the "LAS Dataset to Raster" function, elevation should be selected as the attribute value instead of the reflection intensity. Next, a slope raster should be generated using “Slope” function, with degrees selected as the output measurement. The obtained raster should then be exported to the TIFF format, without forcing the RGB mode. Figure 11 presents an example of roof slopes for Object1.

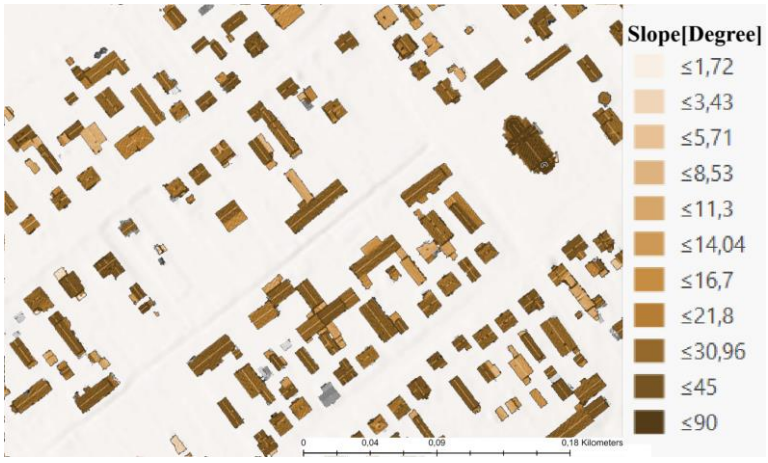

Fig. 11. Example of roof slopes for Object1

The next step (STEP 3.2) involved roof area calculation. Based on the horizontal surface obtained from BDOT10k and the roof slope percentage derived from the point cloud, it is possible to estimate the actual roof surface area:

$$A_{roof} = \frac{A_{building}}{cos\alpha} \tag{4.1}$$

where: A_{roof} - roof area [m^2], $A_{building}$ – building area [m^2], α – the building's roof slope obtained from the point cloud.

During STEP 3.3 if a square meter of asbestos-cement weighs an average of about 14 kg, the tonnage of asbestos can be calculated. Table 2 shows the calculated values of both roof areas and asbestos tonnage. The tonnage estimate is based on horizontal projection.

Table 2. Area and tonnage of asbestos-cement

	Object1	**Object2**	**Object3**
Area [m^2]	48429.62	34509.78	6721.75
Tonnage [kg]	678	483	94

5. Data Validation – STEP 4

To verify the correct operation of the method additional identification parameters was applied, such as: building roof slope and its visual features. Including these parameters in the analysis improves the differentiation of asbestos-cement roofs from other types of roofing.

Eternit was most often used on roofs with moderate to steep slope (15–45°), mainly on gable and multi-pitch structures. On flat roofs, roofing felt predominated, which due to its dark color, may in some cases exhibit reflection intensity similar to eternit. In very rare cases, asbestos-cement boards were also used on flat roofs, most often on small structures such as garages or sheds [14]. Based on this analysis, the validation process allows the exclusion of large and medium-sized flat-roofed buildings, such as apartment blocks, from further consideration.

Roof slope values can be obtained in a relatively simple way: when converting the LAS file to raster format using the "LAS Dataset to Raster" function, elevation should be selected as the attribute value instead of the reflection intensity. The resulting raster should then be exported to the TIFF format, without forcing the RGB mode.

The next step involves assigning slope values to individual buildings, for example those extracted from the BDOT10k topographic database. For this purpose, the Zonal Statistics function in QGIS can be applied, assigning raster-derived values to each object, including the average roof slope.

Using RGB visualizations such as orthophotomaps, satellite images or natural-color point clouds, it is possible to distinguish asbestos-covered roofs, which are characterized by a distinct dark gray color. This feature distinguishes them from other roofing materials, such as sheet metal, which is typically much lighter, or cement roof tiles, which occur in various colors, most commonly red or black. In rare cases, asbestos has been painted, for example red, which can complicate identification. The difference between asbestos-cement and metal roofing is illustrated in Figure 12. The color of asbestos-cement is significantly darker than that of metal roofing, allowing for effective visual differentiation. The circled area highlights a close-up view of the pixels.

Fig. 12. Visual comparison of asbestos and non-asbestos-cement roof

Validation results are presented in Figure 13.

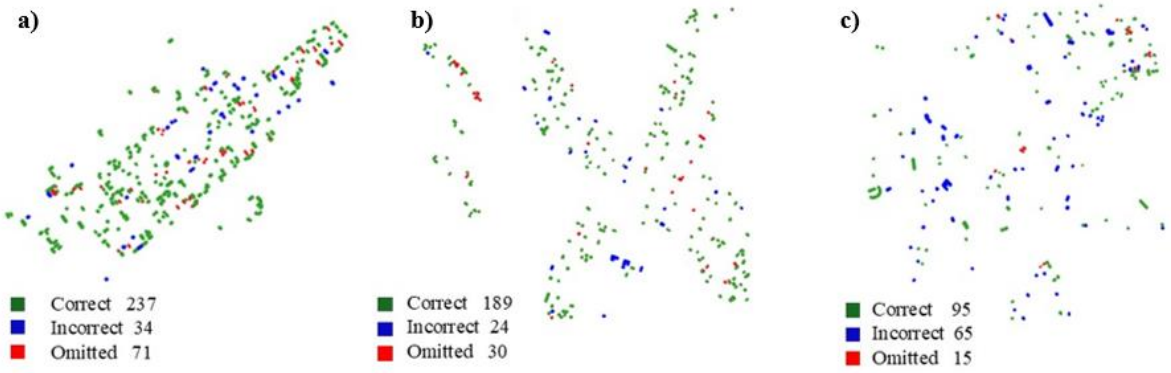

Fig. 13. Validation results, (a) for Object1, (b) for Object2, (c) for Object3

For Object1, the model misclassified about 10% of the buildings and missed 71 others (21% of all structures). For Object2, a similar 10% misclassification rate was observed, while 30 buildings were omitted (12%), indicating slightly better performance than that observed for Object1.

Object3 exhibited the weakest performance: the model misidentified 37% of the buildings and missed 15 (9%). This lower accuracy is likely due to the more complex urban layout and the limited representation of such environments in the training data.

Using the obtained True Positive (correct), False Positive (incorrect), and False Negative (omitted) data, Precision, Recall, F1-score and AP were calculated using "Compute Accuracy for Object Detection" function in ArcGIS Pro, which enables comparison of detected features and ground truth data. Precision indicates the proportion of roofs identified by the model that were correctly classified as asbestos. Recall measures the proportion of all asbestos roofs in the reference data that the model

successfully detected. The F1-score represents the harmonic mean of precision and recall, providing a balanced measure of model performance. The AP metric, ranging from 0 to 1, summarizes model confidence and overall detection quality. The obtained results are shown in Tables 3 and 4.

Table 3. Validation results

Object	True Positive	False Positive	False Negative	Ground-truth	Predicted
Object1	237	34	71	308	271
Object2	189	24	30	219	213
Object3	95	65	15	110	160

Table 4. Accuracy of Object Detection

Object	Precision	Recall	F1 score	AP
Object1	0.87	0.77	0.82	0.76
Object2	0.89	0.86	0.88	0.76
Object3	0.59	0.86	0.70	0.51

Quantitative evaluation demonstrates that the method effectively identifies asbestos-covered buildings across three test areas, achieving precision values ranging from 0.59 to 0.89 and recall values between 0.77 and 0.86. The resulting F1-scores (0.70–0.88) confirm a generally strong balance between correct detections and false alarms. AP values ranged from 0.51 to 0.76, reflecting differences in class separability and data complexity. Object2 exhibited the highest detection quality (precision = 0.89, recall = 0.86, F1 = 0.88), while Object3 showed reduced precision due to a higher rate of false positives (65 cases).

Ground-truth was established through field interviews and subsequently compared to archival ground level photographs, including those available from Google Street View, to address temporal changes between current condition and acquisition dates of available LiDAR data. Although the resulting ground-truth dataset was not perfectly accurate, its quality was considered sufficient for the purposes of this study.

6. DISCUSSION

The erroneous detections result from the frequent occurrence of roofs covered with metal sheets or cement tiles, which have reflectance values similar to asbestos, underscoring the importance of data validation. To illustrate the challenge of unambiguous roof identification, histograms were generated to show the distribution of intensity values for metal sheets and ceramic tiles. These distribution are presented in Figure 14.

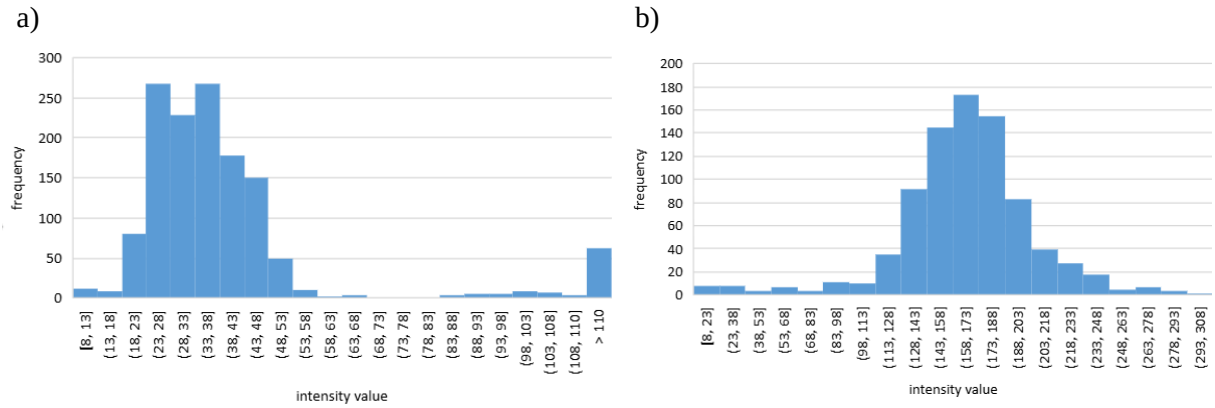

Fig. 14. Histograms, (a) metal sheet roofs, (b) ceramic tiles roofs

An additional characteristic of asbestos-cement sheets is the presence of surface contamination, such as lichens, moss, or dirt deposits. As a result, these roofs may exhibit local brown or green discoloration. For example, a roof covered with lichens may be visible in RGB visualization as a brown spot corresponding to actual location. Figure 15 presents an example of a roof with contaminants that can interfere with the correct identification of the roof covering.

Fig 15. Contamination on asbestos-cement

However, a serious difficulty in identifying asbestos-cement roofing using RGB data is the presence of trees in the immediate vicinity of buildings. Tree canopies may partially cover roofs, causing them to appear green in visualizations. This phenomenon not only makes direct identification difficult but also negatively impacts the effectiveness of machine learning models based on RGB value analysis. The green coloration introduces additional noise, which can cause the model to learn incorrect patterns and, consequently, misclassify buildings covered with other materials as asbestos-covered structures. This issue is illustrated in Figure 16.

Fig. 16. Roof not covered with asbestos-cement, obscured by leaves

A further challenge is the temporal variability of LiDAR acquisitions, which affects both intensity values and the visual appearance of roofs. Differences in acquisition dates, atmospheric conditions, vegetation season, and sensor configurations can modify the recorded reflectance. For instance, LiDAR collected during leaf-on vegetation periods increases the likelihood of partial roof occlusion, whereas winter acquisitions may expose roof surfaces more clearly but alter reflectance due to moisture or residual snow. These temporal factors contribute to inconsistencies that complicate the reliable differentiation between asbestos and other roofing materials.

The misclassification patterns reported in Tables 3 and 4 further confirm the influence of these factors on model performance. In the case of occlusions, roofs partially covered by tree crowns directly contributed to the high number of false negatives observed for all three objects. Similarly, irregular or partially hidden roof shapes increased the number of false positives, particularly for Object3, as reflected in its lower precision value (0.59).

An examination of Tables 3 and 4 shows that similar reflectivity values between asbestos, metal roofing and cement tiles are reflected in the false positive rates. For instance, the high number of false positives corresponds to the significant drop in precision and F1-score. Surface contamination, such as moss or lichen adds further intensity variability, contributing to these observed patterns. Finally, the temporal variability of LiDAR data also helps explain discrepancies between ground-truth and predicted counts. Seasonal differences, moisture levels, or acquisition timing can influence the average precision.

When compared to other methods, such as CNN-based approaches or multispectral/hyperspectral classification, RGB-based and intensity-based detection remains more sensitive to noise, occlusions, and spectral ambiguity. CNNs can better exploit spatial context and texture patterns, while multispectral data provides richer spectral information that enables the separation of materials with similar RGB reflectance. However, these approaches require more complex data sources, greater computational resources, and larger, more diverse training datasets.

7. CONCLUSION

The conducted research indicates that machine learning methods, in combination with LiDAR data and orthophotos, can provide an effective and scalable solution for the identification of asbestos-cement roofing. The developed methodology, based on reflection intensity, roof geometry, and supporting visual and temporal features, demonstrated the potential to create a functional model capable of detecting asbestos-cement roofs with promising, though still improvable, accuracy.

The results suggest that the intensity of laser reflection from asbestos-cement roofs tends to exhibit a characteristic range, which may be utilized as one of the key classification features. Moreover, integrating additional parameters such as roof slope, building age, and visual colour analysis appears to improve detection reliability and reduce the number of false positives.

Although the initial version of the model demonstrated an omission rate of up to 25%, further optimization, especially through the introduction of additional, verified training samples, led to an observed improvement in average precision of nearly 8%. The updated model also indicated improved generalization capabilities and reduced overfitting, enhancing its robustness for broader applications.

Despite some challenges such as vegetation coverage or roofs made of materials with similar reflectivity, this approach shows promise as a valuable tool for supporting large-scale asbestos inventory programs. The method also appears adaptable to various regions, provided proper training data and computational resources are available, thereby reinforcing its practical potential.

Ultimately, the integration of AI-based techniques into environmental monitoring has the potential to accelerate asbestos detection and support public health initiatives by facilitating safer and more targeted removal efforts. This study provides evidence for the potential of remote sensing and machine learning in tackling long-standing environmental hazards in a precise, automated, and cost-effective manner.

Based on the proposed improvements, future research will focus on the development of dedicated models for analyzing roof slope and RGB raster data. Particular emphasis will be placed on implementing a system of weighted parameters, allowing the model to prioritize the most relevant features and thereby enhance classification accuracy. Additionally, further expansion of the training dataset with new, spatially and temporally diverse samples is expected to improve the model's generalization capabilities and robustness against noise.

Future work will also explore the use of transfer learning techniques and the integration of multi-temporal data, which may further improve detection performance under varying environmental conditions. These directions aim to create a more coherent and scalable framework for asbestos-cement roof identification suitable for both regional and national applications.

While the findings are encouraging, they should be interpreted with appropriate caution, as the model's performance may vary depending on regional characteristics and data quality. Therefore, the conclusions represent a promising direction and highlight the importance of ongoing validation and refinement, rather than serving as a definitive solution.

Appendix 1.

Table 5. Background on Machine Learning and GIS Tools

GIS Tool / Function	Software Environment	Purpose in the Study
Point Cloud Download (ALS)	geoportal.gov.pl	Acquisition of Airborne Laser Scanning data used as the primary input for further analysis.
Point Cloud Filtering and Merging	ArcGIS Pro (3D Analyst / LAS Dataset tools)	Cleaning, organizing, and merging ALS point clouds into a unified dataset for raster generation.
LAS Dataset to Raster – Intensity Raster Creation	ArcGIS Pro	Conversion of point cloud intensity values into an RGB TIFF raster used for sample collection and object detection.
Label Objects for Deep Learning	ArcGIS Pro (Image Analyst / Deep Learning tools)	Manual annotation of asbestos-covered roofs and generation of training samples for model development.
Train Deep Learning Model	ArcGIS Pro (Deep Learning framework)	Training a convolution-based model using prepared samples to classify asbestos roofing materials.
Detect Objects Using Deep Learning	ArcGIS Pro	Automatic detection of asbestos-cement roofs on remaining rasters based on the trained model.
LAS Dataset to Raster – Elevation Raster Creation	ArcGIS Pro	Conversion of point cloud elevation data into a height raster for geometric roof analysis.
Slope Tool	ArcGIS Pro (Spatial Analyst)	Computation of roof slope values from the elevation raster.
Zonal Statistics	ArcGIS Pro (Spatial Analyst)	Calculation of horizontal roof areas for buildings detected in the study.
Google Street View	Google Maps	Visual validation of asbestos roofing using archival street-level photographs.

Appendix 2.

Table 6. Parameters which can be used during roof analysis

Parameter Name	Description
Meta Data Format	The format used to record metadata, which describes the data. Metadata is not the data itself but a structured description of it.
Max Epochs	The maximum number of training epochs. One epoch means the entire dataset passes through the neural network once.
Model Type	Specifies the type of deep learning model to be used for training.
Batch Size	The number of training samples processed at one time. A higher batch size may improve performance but require more memory.
Validation %	The percentage of the training data used for validating the model's performance during training.

Chip Size	The size of the image crop used for training. If the image is smaller than this size, the original image size is used.
Learning Rate	The rate at which new information overwrites the existing information during training. If not specified, it is determined automatically from the learning curve.
Backbone Model	A pre-configured neural network architecture used as a base model for training via transfer learning.
Monitor Metric	The metric used to monitor model performance during checkpointing and early stopping.
Weight Initialization Scheme	Specifies how weights are initialized for layers. When using multispectral data, the first layer is reinitialized to support the required input channels.
Freeze Model	Indicates whether the backbone model's layers are frozen to retain their original weights and biases during training.

REFERENCES

1. Tucker, P 2010. Asbestos Toxicity. *Case Studies in Environmental Medicine (CSEM)* Course: WB 1093.
2. Virta, RL 2002. Asbestos: Geology, mineralogy, mining, and uses. *Open-File Report* 02-149.
3. Szymańska, D and Lewandowska, A 2019. Disposal of asbestos and products containing asbestos in Poland. *Journal Material Cycles and Waste Management* **21**, 345–355.
4. Huh, DA, et al. 2022. Disease Latency according to Asbestos Exposure Characteristics among Malignant Mesothelioma and Asbestos-Related Lung Cancer Cases in South Korea. *International Journal of Environmental Research and Public Health*, **19** (23).
5. Rodriguez Elizalde, R 2022. Asbestos Presence in 20th Century Buildings. *Journal of Engineering and Applied Sciences Technology* **4**, 1-14. https://doi.org/10.47363/jeast/2022(4)152.
6. Markowitz SB, et al. 2013. Asbestos, asbestosis, smoking, and lung cancer: New findings from the north American insulator cohort. *American Journal of Respiratory Critical Care Medicine* **188**. https://doi.org/10.1164/rccm.201302-0257OC.
7. Kusiorowski, R, Lipowska B, Kujawa M and Gerle A 2023. Problem of asbestos-containing wastes in Poland. *Cleaner Waste Systems* **4.** https://doi.org/10.1016/j.clwas.2023.100085.
8. Radvanec, M, Lubomír T, Derco J, Čechovská K and Németh, Z 2013. Change of carcinogenic chrysotile fibers in the asbestos cement (eternit) to harmless waste by artificial carbonatization. Petrological and technological results, *Journal of Hazardous Materials* **261**, 252–253. https://doi.org/10.1016/j.jhazmat.2013.02.036.
9. Abbasi M, Mostafa S, Vieira AS, Patorniti N and Stewart, RA 2022. Mapping Roofing with Asbestos-Containing Material by Using Remote Sensing Imagery and Machine Learning-Based Image Classification: A State-of-the-Art Review, *Sustainability* **14**. https://doi.org/10.3390/su14138068.
10. Krówczyńska M, Raczko E, Staniszewska N and Wilk, E 2020. Asbestos-cement roofing identification using remote sensing and convolutional neural networks (CNNs). *Remote Sensing* **12**. https://doi.org/10.3390/rs12030408.

11. López VG, 2021. Programs for Asbestos Abatement. Lessons from Poland, *Archivos de Prevencion Riesgos Laborales* **24**. https://doi.org/10.12961/aprl.2021.24.01.06.
12. Jung, HS et al., 2021. Changes in concentrations and characteristics of asbestos fibers dispersed from corrugated asbestos cement sheets due to stabilizer treatment. Journal of Environmental Management **285**. https://doi.org/10.1016/j.jenvman.2021.112110.
13. Kashani, AG, Olsen, MJ, Parrish, CE and Wilson, N 2015. A review of LIDAR radiometric processing: From ad hoc intensity correction to rigorous radiometric calibration. *Sensors* **15**. https://doi.org/10.3390/s151128099.
14. Janiesch, C, Zschech, P, Heinrich, K, 2021. Machine learning and deep learning. *Electronic Markets* **31**. https://doi.org/10.1007/s12525-021-00475-2.
15. Lundervold, AS, Lundervold, A, 2019. An overview of deep learning in medical imaging focusing on MRI. *Zeitschrift fur medizinische Physik* **29,** 102-127. https://doi.org/10.1016/j.zemedi.2018.11.002.
16. Lukač, N, Seme, S, Žlaus D, Štumberger, G, Žalik, B, 2014. Buildings roofs photovoltaic potential assessment based on LiDAR (Light Detection and Ranging) data. *Renewable Energy* **66**, 1371-1390. https://doi.org/10.1016/j.energy.2013.12.066.
17. Pollino, M et al., 2020. Assessing earthquake-induced urban rubble by means of multiplatform remotely sensed data. ISPRS International Journal of Geo-Information **9**. https://doi.org/10.3390/ijgi9040262